

## Infrared Dielectric Dispersion and Lattice Dynamics of Uranium Dioxide and Thorium Dioxide

J. D. AXE AND G. D. PETTIT

IBM Watson Research Center, Yorktown Heights, New York

(Received 27 April 1966; revised manuscript received 28 June 1966)

Measurements at room temperature of the infrared reflectivity of single crystals of  $\text{ThO}_2$  and  $\text{UO}_2$  have been carried out and analyzed by Kramers-Kronig relations. A single strong resonance is found in each case with  $\omega_{\text{TO}} = 279(\pm 2) \text{ cm}^{-1}$ ,  $\omega_{\text{LO}} = 568(\pm 4) \text{ cm}^{-1}$ ,  $\epsilon_0 - n^2 = 15.5$  for  $\text{ThO}_2$ ;  $\omega_{\text{TO}} = 278(\pm 2) \text{ cm}^{-1}$ ,  $\omega_{\text{LO}} = 556(\pm 4) \text{ cm}^{-1}$ ,  $\epsilon_0 - n^2 = 17.7$  for  $\text{UO}_2$  (TO = transverse optic; LO = longitudinal optic). The best classical dispersion-formula fit to the reflectivity yields the following parameters: for  $\text{ThO}_2$ ,  $\omega_0 = 282.7 \text{ cm}^{-1}$ ,  $\epsilon_0 - n^2 = 14.85$ ,  $\bar{\gamma} = 16.2 \text{ cm}^{-1}$ ; for  $\text{UO}_2$ ,  $\omega_0 = 283.2 \text{ cm}^{-1}$ ,  $\epsilon_0 - n^2 = 15.80$ ,  $\bar{\gamma} = 18.5 \text{ cm}^{-1}$ . The low-frequency (0.3-Mc/sec) dielectric constant of  $\text{ThO}_2$  was measured to be  $18.9 \pm 0.4$ . For  $\text{UO}_2$  the mode frequencies are in excellent agreement with those obtained by neutron spectroscopy, and can be reconciled with existing infrared absorption data by taking into account particle-size corrections which can shift the polar mode frequency by a factor  $\sim (\epsilon_0 + 2/n^2 + 2)^{1/2} \sim 1.8$  for small spherical samples. The above data are used to evaluate (Szigeti-type) effective charges ( $Z'_{\text{Th}^{+4}} = 2.33$ ,  $Z'_{\text{U}^{+4}} = 2.42$ ) and to discuss several approximate relations between the long-wave elastic and optical properties of the fluorite ( $\text{CaF}_2$ -type) lattice. Absorption bands were measured in the two-phonon-combination region in  $\text{UO}_2$  and their assignment is discussed.

### I. INTRODUCTION

BECAUSE of its technological importance, those bulk properties of uranium dioxide ( $\text{UO}_2$ ) of engineering interest are being extensively studied. Because of its relatively simple structure,  $\text{UO}_2$  is of interest from more fundamental points of view as well. Recently Dolling *et al.*<sup>1</sup> have made a study of the lattice dynamics of  $\text{UO}_2$  by inelastic neutron scattering, and are continuing to study antiferromagnetic spin waves by the same techniques.<sup>2</sup> This paper, which concerns itself with the dielectric response of the  $\text{UO}_2$  lattice, supplements to a certain extent the above study. It also supplements optical studies in the near-infrared<sup>3</sup> and visible spectral regions.<sup>4-6</sup> For purposes of comparison we have also made similar measurements on thorium dioxide ( $\text{ThO}_2$ ), which is isomorphous with  $\text{UO}_2$  and proves to have very similar dielectric properties.

In the following section we present the experimental results which were obtained primarily from an analysis of the specular reflectivity of the two materials in the infrared region. This is a very effective technique for obtaining optical constants in lossy spectral regions.

In the Sec. III these results are analyzed in some detail to obtain such parameters as the (Szigeti) effective charge and force constants which are of more fundamental importance in characterizing the lattice dynamics. The interrelationships between various optical, dielectric, and elastic properties of  $\text{UO}_2$  and  $\text{ThO}_2$  are discussed from relations previously derived from a simple shell-model treatment of the long-wavelength

properties of the fluorite lattice.<sup>7</sup> (The fluorite  $\text{CaF}_2$  structure is isomorphous with that of  $\text{UO}_2$  and  $\text{ThO}_2$ .) An elementary discussion of two-phonon absorption processes is attempted in this section also.

One of the reasons for undertaking this work was to attempt to clear up an apparent discrepancy between the existing far-infrared absorption data on dispersed finely powdered samples<sup>8</sup> of  $\text{UO}_2$  and the neutron-scattering data as to the frequency of the fundamental polar mode. Our measurements confirm the neutron results,<sup>1</sup> and we present arguments in support of the conclusion that the shifted absorption frequency reported above is the predictable result of sample sizes small in comparison with the wavelength of the exciting radiation. Under such circumstances, the peaks of the absorption spectra are no longer simply interpretable, at least in terms of resonant frequencies for bulk material.<sup>9-11</sup> The notion of size- and shape-dependent normal modes of this type is not new. Frölich<sup>9</sup> predicted such effects several years ago and related effects have been demonstrated.<sup>10,12</sup>

### II. EXPERIMENTAL

Well characterized single-crystal samples of high quality were used. They were prepared by fusion in an electric-arc furnace and subsequently treated with moist hydrogen at  $1750^\circ\text{C}$ . The materials had 99% theoretical density and the oxygen/metal ratio for the  $\text{UO}_2$  was

<sup>7</sup> J. D. Axe, Phys. Rev. **139**, A1215 (1965).

<sup>8</sup> M. Tsuboi, M. Terada, and T. Shimanouchi, J. Chem. Phys. **36**, 1301 (1962).

<sup>9</sup> H. Frölich, *Theory of Dielectrics* (Oxford University Press, New York, 1948), 2nd ed., pp. 153-155.

<sup>10</sup> M. Hass, Phys. Rev. Letters **13**, 429 (1964).

<sup>11</sup> J. Grindlay, Can. J. Phys. **43**, 1604 (1965). Also A. A. Maradudin and G. H. Weiss, Phys. Rev. **123**, 1958 (1961); H. B. Rosenstock, *ibid.* **121**, 416 (1961); T. H. K. Barron, *ibid.* **123**, 1995 (1961).

<sup>12</sup> D. W. Berreman, Phys. Rev. **130**, 2193 (1963).

<sup>1</sup> G. Dolling, R. A. Cowley, and A. D. B. Woods, Can. J. Phys. **43**, 1397 (1965).

<sup>2</sup> R. A. Cowley and G. Dolling, Bull. Am. Phys. Soc. **11**, 109 (1966).

<sup>3</sup> J. L. Bates, Nucl. Sci. Eng. **21**, 26 (1965).

<sup>4</sup> R. J. Ackermann, R. J. Thorne, and G. H. Winslow, J. Opt. Soc. Am. **49**, 1107 (1959).

<sup>5</sup> A. Companion and G. H. Winslow, J. Opt. Soc. Am. **50**, 1042 (1960).

<sup>6</sup> D. M. Gruen, J. Am. Chem. Soc. **76**, 2117 (1954).

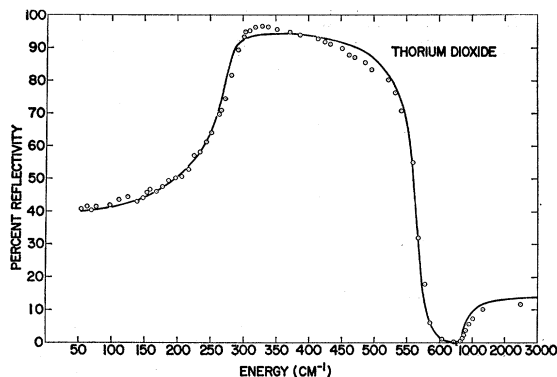


FIG. 1. The infrared reflectivity of  $\text{ThO}_2$ . The circles represent measured points. The solid line represents the reflectivity calculated from the best fitting classical dispersion formula [Eq. (1)]. Note the change of energy scale at  $650\text{ cm}^{-1}$ .

2.001 or better. These samples were prepared at Battelle-Northwest under the direction of Dr. H. J. Anderson.

For reflectivity measurements surfaces of both materials were prepared by standard metallographic procedures, the final polish being on  $.05\text{-}\mu$  alumina. The reflectivity was measured at room temperature and near-normal incidence using point-by-point comparison with an aluminized surface in a Perkin-Elmer model 301 spectrometer. The frequency range between 60 and  $2500\text{ cm}^{-1}$  was covered and the spectral slit widths varied between 1 and  $6\text{ cm}^{-1}$  (see Figs. 1 and 2). The low-frequency dielectric constant (300 kc/sec) for  $\text{ThO}_2$  was determined by measuring the capacitance of a several mm-thick disk of sample material in a conventional Scherring bridge circuit. The conductivity of the

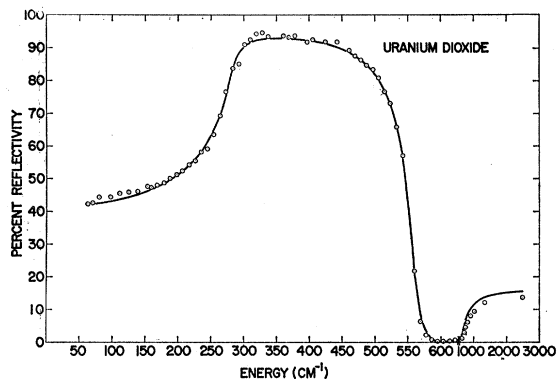


FIG. 2. The infrared reflectivity of  $\text{UO}_2$ . The circles represent measured points. The solid curve represents the reflectivity calculated from the best fitting classical dispersion formula [Eq. (1)]. Note the change of energy scale at  $\sim 650\text{ cm}^{-1}$ .

$\text{UO}_2$  was too high to give a meaningful determination of the low-frequency dielectric constant by this method. It is not believed that this conductivity measurably affected the observed reflectivity.

Two different methods were used to derive the optical constants from the measured reflectivity. The first consisted of a least-squares adjustment of a classical dispersion formula<sup>13</sup>

$$\epsilon(\omega) - n^2 = (\epsilon_0 - n^2)\omega_0^2 / (\omega_0^2 - \omega^2 + i\gamma\omega). \quad (1)$$

Here  $\epsilon_0$  is the static dielectric constant and  $n^2$  represents the dielectric constant at frequencies well above those to which the lattice can respond but below all characteristic electronic excitations.  $\gamma$  is a phenomenological, velocity-dependent damping term. The best-fitting reflectivities of this form are shown as the solid lines in Figs. 1 and 2. Similarly, the solid lines in Figs. 3 and 4 represent the real and imaginary parts of the refractive index as given by Eq. (1) for the best-fitting parameters. The parameters thus obtained are given in Table I. The second method made use of the Kramers-Kronig relation between  $R(\omega)$ , the fraction of reflected energy at a given frequency, and the phase shift,  $\theta(\omega)$ , which

TABLE I. Some quantities related to the elastic and infrared dielectric properties of  $\text{ThO}_2$  and  $\text{UO}_2$ .

	$\text{ThO}_2$	$\text{UO}_2$
Kramers-Kronig analysis		
$\omega_{\text{TO}}(\text{cm}^{-1})$	$279(\pm 2)$	$278(\pm 2)$
$\omega_{\text{LO}}(\text{cm}^{-1})$	$568(\pm 4)$	$556(\pm 4)$
$(\epsilon_0 - n^2)$	15.5	17.7
Classical dispersion analysis		
$\omega_0(\text{cm}^{-1})$	282.7	283.2
$(\epsilon_0 - n^2)$	14.85	15.80
$n^2$	4.86	5.51
$\bar{\gamma}(\text{cm}^{-1})$	16.2	18.5
Measured dielectric constants		
$\epsilon_0$	$18.9(\pm 0.4)$	$24^a$
$n^2$	$4.30(\pm 0.05)^b$	$5.3^b$
$(\epsilon_0/n^2)$	4.39	4.53
$(\omega_{\text{LO}}/\omega_{\text{TO}})^2$	4.14	4.00
Effective charge $Z'_M{}^{4+}(e)$		
$R_{M0}(10^4\text{ cm-dyn}^{-1})$	-21.2	-23.1
$\beta_{\text{obs}}(10^{-12}\text{ cm}^2\text{-dyn})$	0.518 <sup>c</sup>	0.472 <sup>d</sup>
$\beta_{\text{calc}}^e$	...	0.478

<sup>a</sup> A. Briggs, Report to the International Atomic Energy Agency, Vienna (unpublished).

<sup>b</sup> Reference 18.

<sup>c</sup> P. M. Macedo, W. Capps, and J. B. Wachtman, Jr., J. Am. Ceram. Soc. **47**, 12 (1964).

<sup>d</sup> J. B. Wachtman, M. L. Wheat, H. J. Anderson, and J. L. Bates, J. Nucl. Energy (to be published).

<sup>e</sup> Equation (8).

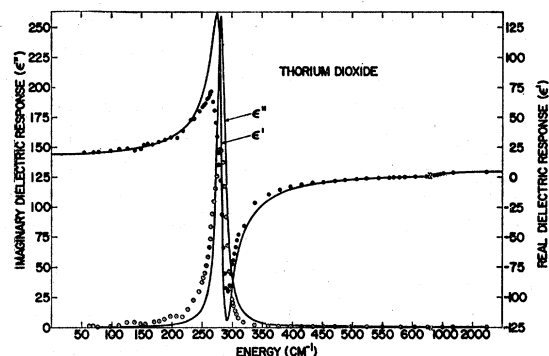


FIG. 3. The infrared dielectric response of  $\text{ThO}_2$ . The circles represent values calculated by the Kramers-Kronig relation [Eq. (2)]. The solid curve represents the best fitting classical dispersion formula [Eq. (1)].

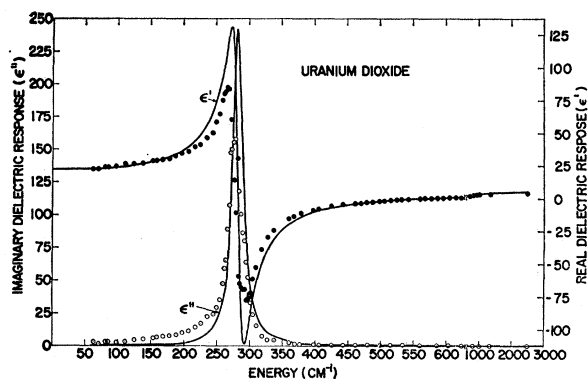


FIG. 4. The infrared dielectric response of  $\text{UO}_2$ . The circles represent values calculated by the Kramers-Kronig relation [Eq. (2)]. The solid curve represents the best fitting classical dispersion formula [Eq. (1)].

occurs upon reflection<sup>13</sup>

$$\theta(\omega) = \left(\frac{2\omega}{\pi}\right) \int \frac{d\omega'}{(\omega^2 - \omega'^2)} \ln \left[ \frac{R(\omega')}{R(\omega)} \right]. \quad (2)$$

Once  $\theta(\omega)$  is known it is possible to rigorously deduce all the optical constants of interest. Both the numerical integration of Eq. (2) and the subsequent calculations of the optical constants were performed for each data point using an IBM 7094 digital computer.<sup>14</sup> The results for the real and imaginary dielectric constants computed in this manner are shown in Figs. 3 and 4. It is possible that the large discrepancy between the dielectric response as deduced by the two methods around  $\omega_0$  is a measure of the difference between the true frequency-dependent damping function  $\gamma(\omega)$ <sup>15,16</sup> and the constant average value  $\bar{\gamma}$ , determined by the fit to the reflectivity. As can be seen from Table I, the two methods are substantially in agreement as to both the position and total strength,  $\epsilon_0 - n^2$ , of the resonance.

At energies greater than about 600  $\text{cm}^{-1}$  it was possible to study the transmission of thin ( $x \geq 50 \mu$ ) wafers of  $\text{UO}_2$  at both 300 and 77°K. When corrected for reflection losses according to the expression<sup>17</sup>  $T = [(1-R)^2 e^{-\alpha x}] / [1 - R^2 e^{-2\alpha x}]$  these data yielded the absorption coefficients  $\alpha$  given in Fig. 5. Bates<sup>9</sup> has published absorption measurements which are qualitatively similar in the 3000- to 900- $\text{cm}^{-1}$  region, but show more pronounced discrepancies at lower energies. The absorption coefficient predicted from the best-fitting damped-oscillator model [Eq. (1)] has been included in the figure as well. It is somewhat surprising that the absorption constants derived from the reflec-

tivity measurements hold so well so far out in the wings ( $\alpha_{\text{max}} \approx 3.6 \times 10^4 \text{ cm}^{-1}$ ). (Although not included in Fig. 5, absorption constants derived from the Kramers-Kronig analysis of the reflectivity agree about equally well over most of this region.)

### III. DISCUSSION

Symmetry arguments support the experimental observation of a single, strong infrared resonance in the fluorite structure. The uranium-dioxide lattice consists of three inter-penetrating face-centered-cubic (fcc) lattices, with spacing  $2r_0$ . The two oxygen sublattices are at  $(\frac{1}{4}, \frac{1}{4}, \frac{1}{4})(2r_0)$  and  $(-\frac{1}{4}, -\frac{1}{4}, -\frac{1}{4})(2r_0)$  relative to the uranium sublattice. The long-wavelength ( $k=0$ ) excitations consist of motions of these rigid sublattices against one another. The nine possible such degrees of freedom must form bases for  $2F_{1u} + F_{2g}$  irreducible representations of the point group  $O_h(m3m)$ . The Raman active  $F_{2g}$  vibrations can be shown to involve equal and opposite motions of the oxygen sublattices only and do not affect the dielectric dispersion in first order because there is no net dipole moment within the unit cell. One set of  $F_{1u}$  normal coordinates represent the acoustic branches. The degeneracy of the remaining  $F_{1u}$  set near  $k=0$  is partially lifted because of the macroscopic electric field associated with its longitudinal component.

The frequency of the transverse branch is given by the pole of the complex dielectric response,  $\epsilon(\omega_{\text{TO}}) = \infty$ , whereas the frequency of the longitudinal branch is fixed at the (high-frequency) root,  $\epsilon(\omega_{\text{LO}}) = 0$ . Omitting second-order corrections due to damping,  $\omega_{\text{TO}}$  is given by the peak of the imaginary response,  $\epsilon''_{\text{max}}(\omega) = \epsilon''(\omega_{\text{TO}})$ , and  $\omega_{\text{LO}}$  by the upper root of the real response,  $\epsilon'(\omega_{\text{LO}}) = 0$ . These characteristic frequencies as determined from the Kramers-Kronig analysis of the  $\text{ThO}_2$  and  $\text{UO}_2$  are given in Table I. Also the total ionic contributions to the static dielectric constant

$$(\epsilon_0 - n^2)_{\text{KK}} = \left(\frac{2}{\pi}\right) \int d\omega \frac{\epsilon''(\omega)}{\omega} \quad (3)$$

determined by numerical integration, are given.

The measured values of the high- and low-frequency dielectric constants provide a check on the validity of

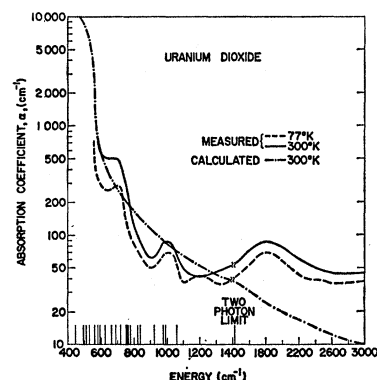


FIG. 5. The absorption coefficients of  $\text{UO}_2$  in the two-phonon absorption region. The calculated values are obtained from the best fitting classical dispersion formula [Eq. (1)]. The markers on the lower left indicate the energy of some of the critical points occurring at special positions on the Brillouin zone boundary (see text).

<sup>13</sup> F. Stern, in *Solid State Physics*, edited by F. Seitz and D. Turnbull (Academic Press Inc., New York, 1963), Vol. 15, p. 333.

<sup>14</sup> Some additional details of experimental techniques and equipment and data reduction have been published in an earlier paper: J. D. Axe, J. W. Gaglianella, and J. E. Scardefield, *Phys. Rev.* **139**, A1211 (1965).

<sup>15</sup> See, for example, M. Lax, *J. Phys. Chem. Solids* **25**, 487 (1964).

<sup>16</sup> H. Bilz, L. Genzel, and H. Happ, *Z. Physik* **160**, 535 (1960).

<sup>17</sup> In making these corrections the reflectivity was assumed to be temperature-independent.

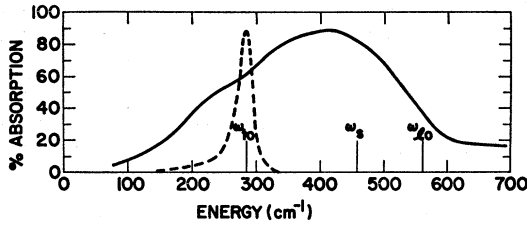


FIG. 6. A comparison of the observed absorption of  $\text{UO}_2$  dispersed in polyethylene (solid curve) with the LO and TO mode frequencies for a large sample and with the mode frequency  $\omega_s$  calculated for a small spherical particle (see text). The dashed curve, proportional to the imaginary dielectric response, is included to show the intrinsic linewidth.

the Lyddane-Sachs-Teller (LST) relation  $(\epsilon_0/n^2) = (\omega_{\text{LO}}/\omega_{\text{TO}})^2$ . As can be seen from Table I the agreement is considerably worse for the  $\text{UO}_2$  than for the  $\text{ThO}_2$ . In fact there is considerable dispersion in the refractive index of  $\text{UO}_2$  at visible frequencies<sup>18</sup> and it is likely that an even lower extrapolated value of  $n^2$  should be used although there seems to be no simple unambiguous procedure for performing the extrapolation. This would have the effect of further accentuating the lack of agreement with the Lyddane-Sachs-Teller relation. Deviations of this order can perhaps be realized through anharmonic lattice potentials.<sup>19</sup> An additional factor to be considered in the case of  $\text{UO}_2$  is the influence of low-lying electronic states of the uranium ion.<sup>20</sup> Electronic effects which may violate the adiabatic assumption of the LST relation would be of an indirect nature in  $\text{UO}_2$ , since electric-dipole transitions between these low-lying levels are forbidden by parity. (See below for additional experimental indication of the possible position of these low-lying electronic levels.)

The fluorite lattice can be partially characterized in terms of parameters which appear in expressions exactly analogous to the Szigeti relations<sup>21,22</sup> for lattices with diatomic unit cells. A shell-model treatment of the fluorite lattice yields<sup>7</sup>

$$Z_M' Z_O' = -(9v/4\pi e^2) [(\epsilon_0 - n^2)/(n^2 + 2)^2] \mu_0 \omega_{\text{TO}}^2, \quad (4)$$

$$R_{MO}' = -[(\epsilon_0 + 2)/(n^2 + 2)] \mu_0 \omega_{\text{TO}}^2 \quad (5)$$

$Z_O'$  and  $Z_M' = -2Z_O'$  are the Szigeti effective charges,  $R_{MO}'$  is the effective short-range force constant between  $M$ - $O$  nearest neighbors and  $\mu_0$  is the appropriate reduced mass  $m_M m_O / [m_M + 2m_O]$ . If the assumption of central forces is made a simple relationship between the  $k=0$  optical-mode frequencies and the lattice compressibility

$\beta$  exists, then

$$\beta^{-1} = \left(\frac{1}{3}\right) (c_{11} + 2c_{12}) = (12r_0)^{-1} \times \{2[(\epsilon_0 + 2)/(n^2 + 2)] \mu_0 \omega_{\text{TO}}^2 + \mu_R \omega_R^2\}. \quad (6)$$

Here  $2r_0$  is the cubic-unit-cell spacing,  $\mu_R = m_O$  and  $\omega_R$  being, respectively, the reduced mass and frequency characteristic of the Raman active mode. [Small shell-model polarization corrections have been omitted in Eq. (3)]. The values of these quantities derived for  $\text{ThO}_2$  and  $\text{UO}_2$  are given in Table I. When compared to the values for the alkaline-earth fluorides the present effective charges are not doubled, as might be expected, but are increased by some 40%; the force constants are roughly doubled. This may be a measure of the increased importance of short-range polarization in the oxide, or increased covalency, or both. The agreement between the measured compressibility of  $\text{UO}_2$  and that calculated by Eq. (6) is excellent.

There has recently been considerable interest in the interpretation of the fine structure generally seen on the short-wavelength lattice absorption edge in terms of a process whereby two phonons are created at the expense of a single infrared photon.<sup>23-27</sup> Wave-vector conservation requires that the two phonons be characterized by equal but opposite wave vectors, and the absorption features then reflect the singularities in the density of  $(+\mathbf{k}, -\mathbf{k})$  pair states of the participating phonons. Even for the relatively simple  $\text{UO}_2$  structure, the nine phonon branches give rise to 36 two-phonon combination branches for a general  $|\mathbf{k}|$ ,<sup>28</sup> and just the evaluation of the number and type of critical points is an undertaking which hardly seems worthwhile in view of the smooth appearance of the data in Fig. 4. To emphasize this point, Fig. 4 also includes the frequencies of what are but a few of the possible critical points at special symmetry points on the zone boundary. These frequencies have been measured by Dolling *et al.*<sup>1</sup> The formal complexity of the situation does not obscure one assignment, however. Inspection of the dispersion curves of Ref. 1 discloses that the  $\omega(\mathbf{k})$  surface which at  $\mathbf{k}=0$  is associated with the longitudinal, optically active mode intersects the critical points  $M$  and  $L$  on the zone boundary at nearly the same frequency,  $590(\pm 17)\text{cm}^{-1}$ . This may be taken as an indication that the surface intersects the whole zone boundary at about this frequency which we denote for simplicity as  $\omega_{\text{LO}}$ . A similar state of affairs exists for the surface representing the transverse Raman active branch, the characteristic frequency being  $\omega_{\text{TR}}' = 431(\pm 25)\text{cm}^{-1}$ . Phonon branches of this type which show

<sup>18</sup> W. P. Ellis, J. Opt. Soc. Am. **54**, 265 (1964). The dispersion in  $\text{ThO}_2$  is considerably less in the visible region [see W. P. Ellis and R. M. Lindstrom, Opt. Acta **11**, 287 (1964)], and can be represented by the simple expression  $n^2 - 1 = c[1 - (\lambda_0/\lambda)^2]^{-1}$  with  $\lambda_0 = 0.117 \mu$  and  $c = 3.30$ .

<sup>19</sup> R. A. Cowley, Advan. Phys. **12**, 421 (1963).

<sup>20</sup> R. A. Satten, C. L. Schreiber, and E. Y. Wong, J. Chem. Phys. **42**, 162 (1965).

<sup>21</sup> B. Szigeti, Proc. Roy. Soc. (London) **A204**, 51 (1950).

<sup>22</sup> M. Born and K. Huang, *Dynamical Theory of Crystal Lattices* (Oxford University Press, New York, 1954).

<sup>23</sup> H. Bilz and L. Genzel, Z. Physik **162**, 53 (1962).

<sup>24</sup> M. Lax and E. Burstein, Phys. Rev. **97**, 39 (1955).

<sup>25</sup> J. L. Birman, Phys. Rev. **131**, 1489 (1963).

<sup>26</sup> W. J. Turner and W. E. Reese, Phys. Rev. **127**, 126 (1962).

<sup>27</sup> F. A. Johnson and R. Loudon, Proc. Roy. Soc. (London) **A281**, 274 (1964).

<sup>28</sup> When the two phonons in the pair belong to different single-phonon branches, the result is known as a combination branch. Overtone branches (two phonons from the same branch) are not infrared active in crystals with inversion symmetry.

little dispersion along the zone boundary should be associated with sharp peaks in both the single and combined densities of states. The frequency of the observed peak at about  $1010\text{ cm}^{-1}$  agrees quite well with  $\omega_{\text{LO}'} + \omega_{\text{TR}'}$ . The intensity of this two-phonon absorption should vary with temperature as  $[1 + n(\omega_{\text{TR}'}) + n(\omega_{\text{LO}'})]$ . This predicts a ratio  $\alpha_{300^\circ}/\alpha_{77^\circ} = 1.4$  at  $\sim 1000\text{ cm}^{-1}$ , which is in reasonable agreement with observation. Finally we note that the highest phonon frequency in  $\text{UO}_2$  calculated by Dolling *et al.* is about  $700\text{ cm}^{-1}$ . Therefore the rather broad absorption centered at about  $1800\text{ cm}^{-1}$  cannot be due to two-phonon absorption and seems too strong to be accounted for by higher order multiple-phonon processes. This suggests that it is electronic in origin, possibly due to magnetic-dipole transitions between states of the  $5f^2$  configuration of  $\text{U}^{4+}$ .

Upon superficial examination, the far-infrared-absorption measurements on  $\text{UO}_2$  by Tsuboi *et al.*<sup>8</sup> seem inconsistent with the present results. The result obtained by these workers on fine powdered samples dispersed in a polyethylene film is shown in Fig. 6. It is immediately apparent that the absorption is centered about a frequency ( $412\text{ cm}^{-1}$ ) considerably shifted from the value of  $\omega_{\text{TO}}$  as observed by neutron scattering and confirmed by our dielectric-dispersion analysis. Also the absorption is spread over several hundred  $\text{cm}^{-1}$ , whereas our dielectric-response data indicate a linewidth of about  $25\text{ cm}^{-1}$ . We believe that this result can be largely understood as a manifestation of the shape-dependent frequency of long-wavelength modes. That such effects as we are to describe should exist was first pointed out by Frölich,<sup>9</sup> but in spite of this and more recent work,<sup>10,11</sup> the effect is not widely appreciated among infrared spectroscopists who are accustomed to thinking of their measurements as pertaining to intrinsic microscopic phenomena, and who routinely use methods similar to those described above in examining dispersed powdered samples.

Qualitatively the explanation lies in the fact that the dipole moment accompanying long-wavelength polar phonons gives rise to macroscopic electric fields, which for large samples (containing many wavelengths of excitation) provide additional restoring forces for longitudinal modes and increase their frequencies relative to transverse modes. The fundamental modes of particles of comparable or smaller dimensions than the natural excitation wavelengths can no longer be classified into longitudinal and transverse, and the mode frequencies become dependent upon the size and shape of the particles, but are constrained to lie roughly within a region  $\omega_{\text{TO}} \leq \omega \leq \omega_{\text{LO}}$ . For weak transitions e.g., combination or overtone bands, the difference between  $\omega_{\text{TO}}$  and  $\omega_{\text{LO}}$  is slight. However, for long-wavelength fundamental absorption, the ratio  $\omega_{\text{LO}}/\omega_{\text{TO}}$  can be two or more, and small-particle absorption spectra will consist of contributions of modes distributed over

a wide range of frequencies and not directly interpretable in terms of mode frequencies of macroscopic samples.

The easiest case to discuss quantitatively is that of a spherical sample with radius  $r \ll \lambda$ , the wavelength of the exciting radiation. On the basis of a simple model of a cubic ionic crystal with one infrared active mode, Frölich has shown that the lowest energy mode is a triply degenerate one of uniform polarization (and is therefore infrared active) with a frequency related to the frequency of the macroscopic sample  $\omega_{\text{TO}}$  by the relation  $\omega_s^2 = \omega_{\text{TO}}^2(\epsilon_0 + 2/n^2 + 2)$ . It is a simple matter to rederive this relationship for a small spherical sample embedded in a homogeneous dielectric medium with a dielectric constant  $\epsilon_M$ . The result is  $\omega_s^2 = \omega_{\text{TO}}^2(\epsilon_0 + 2\epsilon_M/n^2 + 2\epsilon_M)$ . As a reference point we have included this small sphere eigenfrequency  $\omega_s = 457\text{ cm}^{-1}$  calculated for  $\text{UO}_2$  in polyethylene ( $\epsilon_M = 2.0$ ). This model is oversimplified in several important respects; nevertheless we feel that the above considerations provide a plausible explanation of the apparent incompatibilities in the existing optical data on  $\text{UO}_2$  and serve at the same time as warning of the pitfalls possible in interpreting data on finely divided samples.

#### IV. SUMMARY

Measurements of the infrared reflectivity of  $\text{UO}_2$  and  $\text{ThO}_2$ , supplemented with static dielectric constant and near-infrared absorption measurements are used to provide the basis for a rather detailed discussion of the long-wavelength lattice dynamics of these materials. The frequencies of both the longitudinal and transverse optically active modes are obtained and for  $\text{UO}_2$  they are in excellent agreement with those found by inelastic neutron scattering. The discrepancy between these results and previous absorption measurements on finely divided  $\text{UO}_2$  particles is discussed. The principle source of discrepancy is shown to be the correction to the long-wavelength polar-mode frequencies in small particles.

The Lyddane-Sachs-Teller relation seems less well obeyed in  $\text{UO}_2$ , which has low-lying electronic levels than in  $\text{ThO}_2$ . The Szigeti effective charges are about 60% of the formal ionic charges. The measured compressibility of  $\text{UO}_2$  is in good agreement with that calculated from the optical-mode frequencies using a Szigeti-type relation. It does not seem profitable at the present time to analyze in detail the two-phonon absorption seen above the fundamental resonance in  $\text{UO}_2$ . However, one band is readily identifiable in terms of a combination of two average phonon frequencies at the Brillouin-zone edge observed by neutron-scattering experiments.

#### ACKNOWLEDGMENTS

The authors wish to thank H. J. Anderson and Battelle-Northwest for generously providing the  $\text{UO}_2$  and  $\text{ThO}_2$  single crystals which made this work possible.